Supplementary Information

Nanostructured Manganese Oxides Exhibit Facet-Dependent Oxidation Capabilities

Di Fu[†], *Lin Duan*[*†], *Chuanjia Jiang*[†], *Tong Zhang*[†], *Wei Chen*[*†]

[†] College of Environmental Science and Engineering, Ministry of Education Key Laboratory of Pollution Processes and Environmental Criteria, Tianjin Key Laboratory of Environmental Remediation and Pollution Control, Nankai University, 38 Tongyan Road, Tianjin 300350, China

Manuscript prepared for *Environmental Science: Nano*

* Corresponding author: (Phone/fax) 86-22-85358169; (E-mail) duanlin@nankai.edu.cn, chenwei@nankai.edu.cn.

Number of pages: 13

Number of figures: 7

Synthesis of α-MnO_2 nanostructures

The two α-MnO_2 nanostructures were synthesized with methods modified from those reported by Rong et al.[1] α-MnO_2-100 was synthesized as follows: firstly, 40 mmol L^{-1} of $KMnO_4$ and 10 mmol L^{-1} of $(NH_4)_2SO_4$ were dissolved in 70 mL of deionized water under continuous magnetic stirring at room temperature for 30 min. The mixture solution was then transferred into a 100-mL Teflon-lined stainless-steel autoclave and maintained at 180 °C for 24 h. After the autoclave cooled naturally to room temperature, the dark brown precipitates were collected by centrifugation, then washed several times with deionized water, and finally dried at 60 °C. α-MnO_2-310 was synthesized similarly, except that $(NH_4)_2C_2O_4$ was used instead of $(NH_4)_2SO_4$.

Analysis of oxidation products of bisphenol A

The aqueous solutions containing BPA oxidation products were filtrated through a 0.22-μm membrane filter, and extracted by trichloroethane. The extracts were concentrated at room temperature (25.0 ± 0.5 °C), diluted to 1 mL with methanol, and then analyzed by UPLC-MS/MS equipped with an Acquity UPLC BEH C18 column (1.7 μm, 2.1 × 50 mm) (XEVO-TQS, Waters, USA). The mobile-phase was methanol with a flow rate of 0.45 mL/min. The mass spectrometer was operated in the *m*/*z* 50-500 range for UPLC-MS/MS. The cone voltage was set to 40 V. The desolvation temperature and source temperature were 350 and 150 °C, respectively.

Density functional theory (DFT) calculation

First-principles calculations were performed by employing the Vienna ab-initio simulation package (VASP). The core-valence interaction was represented by the projector-augmented wave (PAW) method.[2, 3] The cut-off energy was set at 450 eV for the plane-wave basis

restriction. The generalized gradient approximation (GGA) with the Perdew-Burke-Ernzerhof (PBE) was used to describe exchange-correlation functional. Local Hubbard parameter *U* correction was applied in the calculations with a *U* value of 5.2 for Mn.[1] The Brillouin-zone integration was sampled with the K-points according to the Monkhorst-Pack scheme for α-MnO_2 surfaces. The energy criterion for convergence of the electron density was set at 10^{-5} eV, and the force criterion was set at 0.05 eV/Å. A vacuum slab of 20 Å was applied for surface isolation to prevent interactions between two adjacent surfaces for all surface models. Three surface layers were relaxed and all other atoms were fixed to simulate the bulk structure.

The undissociated BPA molecule, which is the predominant species under the experimental conditions, was used in the calculations. To account for the effect of water on the adsorption of BPA (i.e., the polar interactions of water molecules with BPA and with MnO_2), one water molecule was placed in the systems and was allowed to form hydrogen bonding with BPA, or with the α-MnO_2 surface. Note that for α-MnO_2 the bidentate complex on the {100} facets formed with Mn_{4c} atoms was selected in the DFT calculations, rather than Mn_{5c} atoms, because higher adsorption energy to form monodentate complex was observed between Mn_{4c} atoms and the BPA molecules than that of Mn_{5c} atoms; similarly, calculations were conducted for the bidentate complex on the {310} facets formed with Mn_{3c} atoms, rather than Mn_{5c} atoms. The adsorption energies (ΔE_{ads}) were calculated as follows:

$$\Delta E_{ads} = E_{slab + H_2O + BPA} - (E_{slab} + E_{H_2O} + E_{BPA}) \quad \text{(S1)}$$

where $E_{slab + H_2O + BPA}$, E_{slab}, E_{H_2O}, and E_{BPA} are the total energy of the optimized slab model with a H_2O molecule and a BPA surface complex, the energy of the initial slab model surface, the energy of a H_2O molecule and the energy of a BPA molecule, respectively.

Reaction scheme of phenols oxidation by manganese oxides

The oxidation of phenols by manganese oxides includes the following steps:[4]

Precursor complex formation:

$$> Mn^{III/IV} + ArOH \rightleftharpoons (> Mn^{III/IV}, ArOH) \quad (S2)$$

Electron transfer:

$$(> Mn^{III/IV}, ArOH) \rightleftharpoons (> Mn^{II}, ArO\cdot) + H^{+} \quad (S3)$$

Release of phenoxy radical:

$$(> Mn^{II}, ArO\cdot) \rightleftharpoons > Mn^{II} + ArO\cdot \quad (S4)$$

Release of reduced Mn(II):

$$> Mn^{II} \rightleftharpoons > Mn^{2+} \quad (S5)$$

Coupling and further oxidation:

$$ArO\cdot + ArO\cdot \rightarrow \text{quinones, dimers, and polymeric oxidation products} \quad (S6)$$

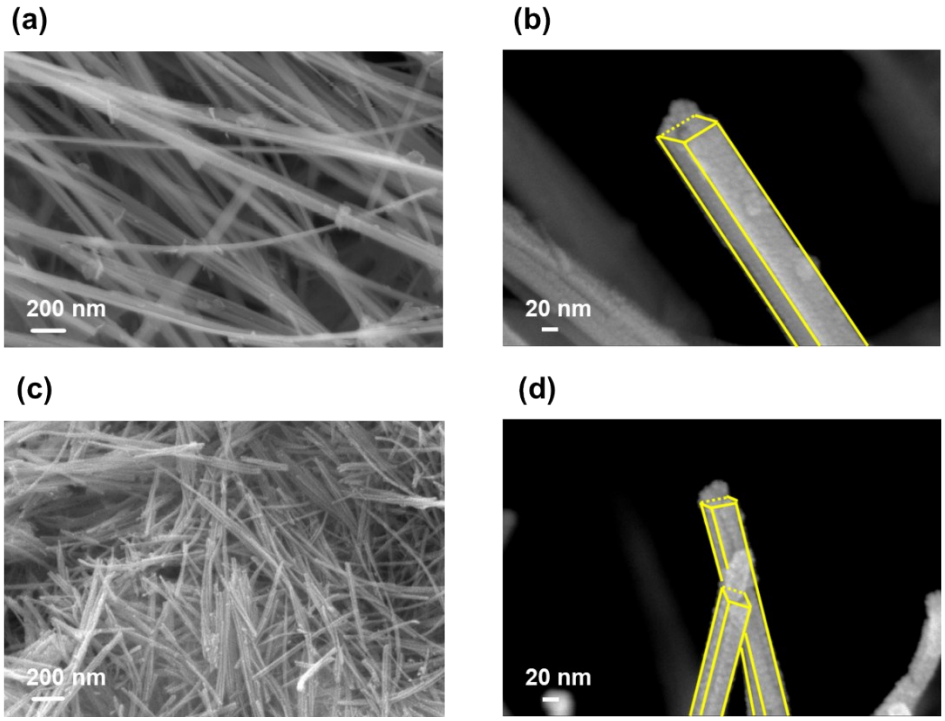

Fig. S1 SEM images of (a, b) α-MnO_2-100 and (c, d) α-MnO_2-310.

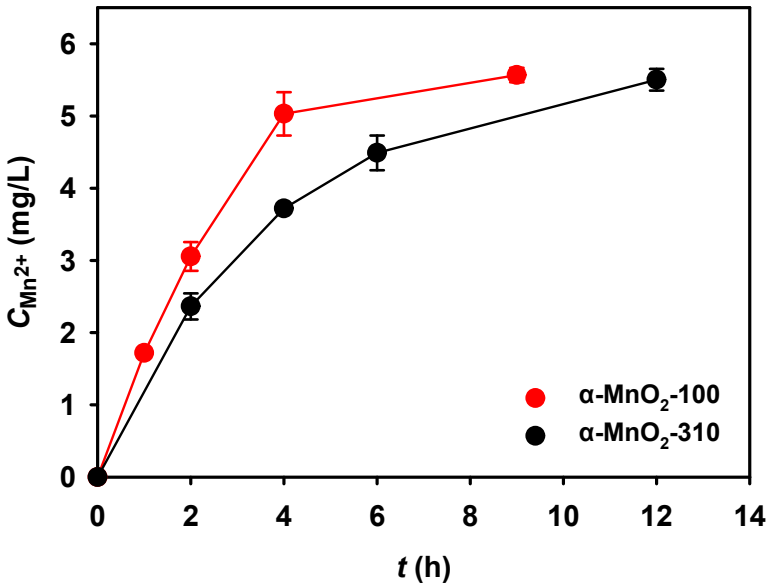

Fig. S2 Release kinetics of dissolved Mn^{2+} during the oxidation of BPA by α-MnO_2-100 and α-MnO_2-310. $[BPA]_0$ = 10 mg L^{-1}, $[\alpha\text{-}MnO_2]_0$ = 35 mg L^{-1}. Error bars indicate variances of duplicates.

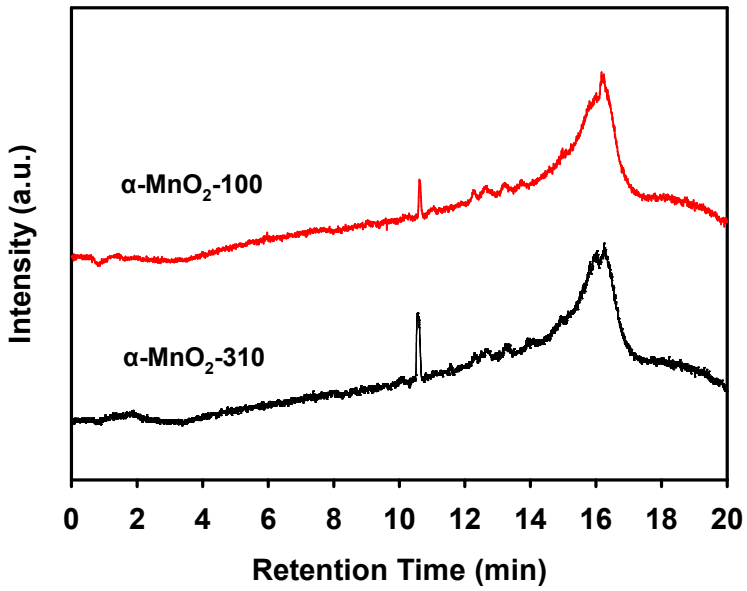

Fig. S3 Total ion chromatogram (TIC) of BPA and its reaction products by α-MnO_2-100 and α-MnO_2-310.

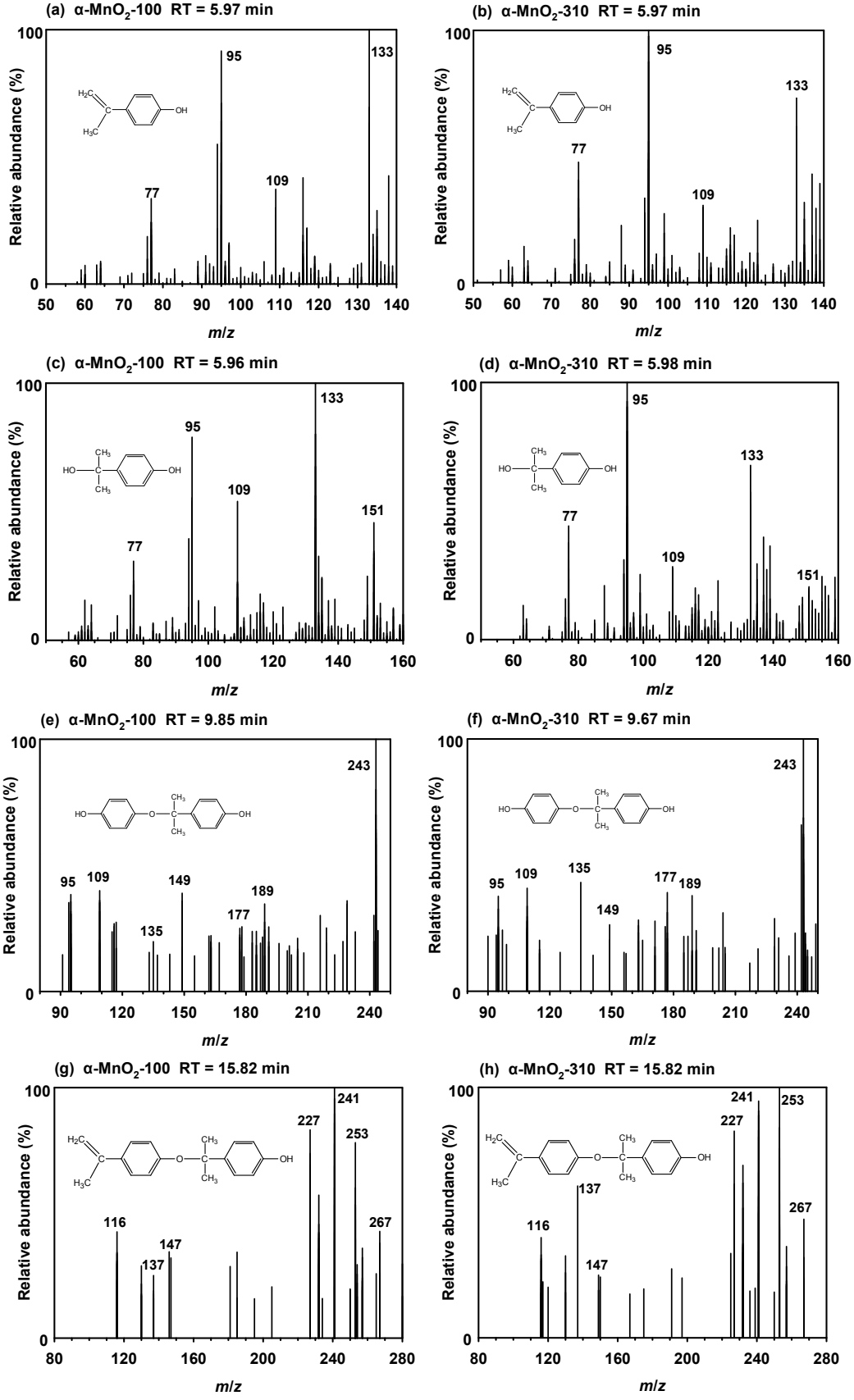
(a) α-MnO2-100 RT = 5.97 min
(b) α-MnO2-310 RT = 5.97 min
(c) α-MnO2-100 RT = 5.96 min
(d) α-MnO2-310 RT = 5.98 min
(e) α-MnO2-100 RT = 9.85 min
(f) α-MnO2-310 RT = 9.67 min
(g) α-MnO2-100 RT = 15.82 min
(h) α-MnO2-310 RT = 15.82 min
Relative abundance (%)
m/z

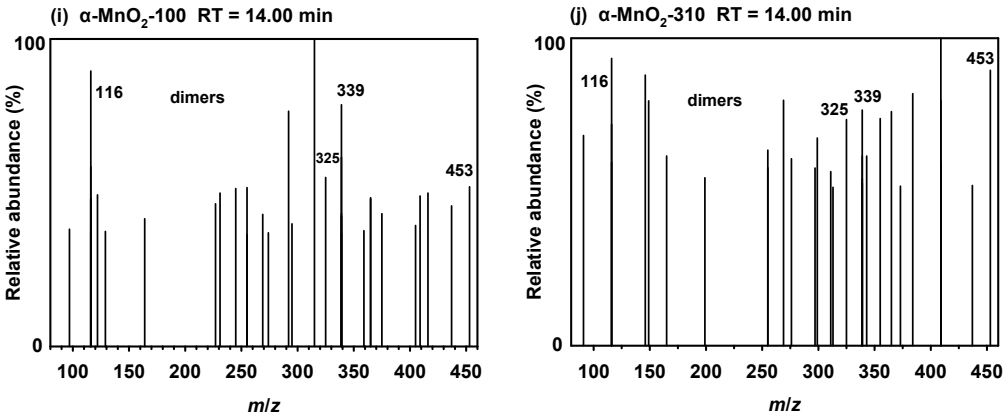

Fig. S4 Mass spectra of identified BPA reaction products by (a, c, e, g, i) α-MnO_2-100 and (b, d, f, h, j) α-MnO_2-310, respectively.

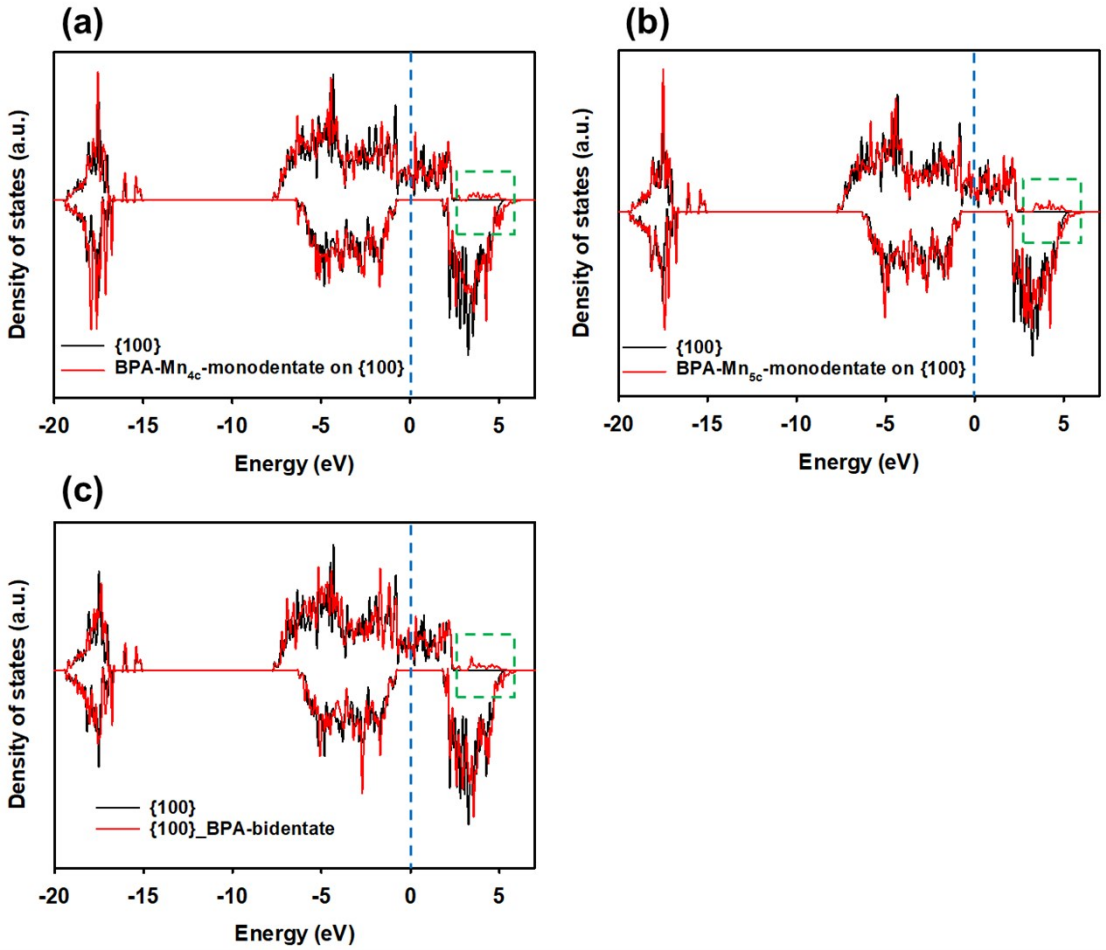

Fig. S5 Total density of states (TDOS) of α-MnO_2 surfaces exposed with the {100} facet before and after BPA adsorption in different complexation configurations: (a) monodentate coordination to Mn_{4c}, (b) monodentate coordination to Mn_{5c}, (c) bidentate coordination. The vertical blue dashed lines represent the Fermi level. New peaks (in green dashed frame) were observed at 2.5-5.0 eV in the valence band (VB) after BPA adsorption, indicating the formation of stable adsorption complexes.

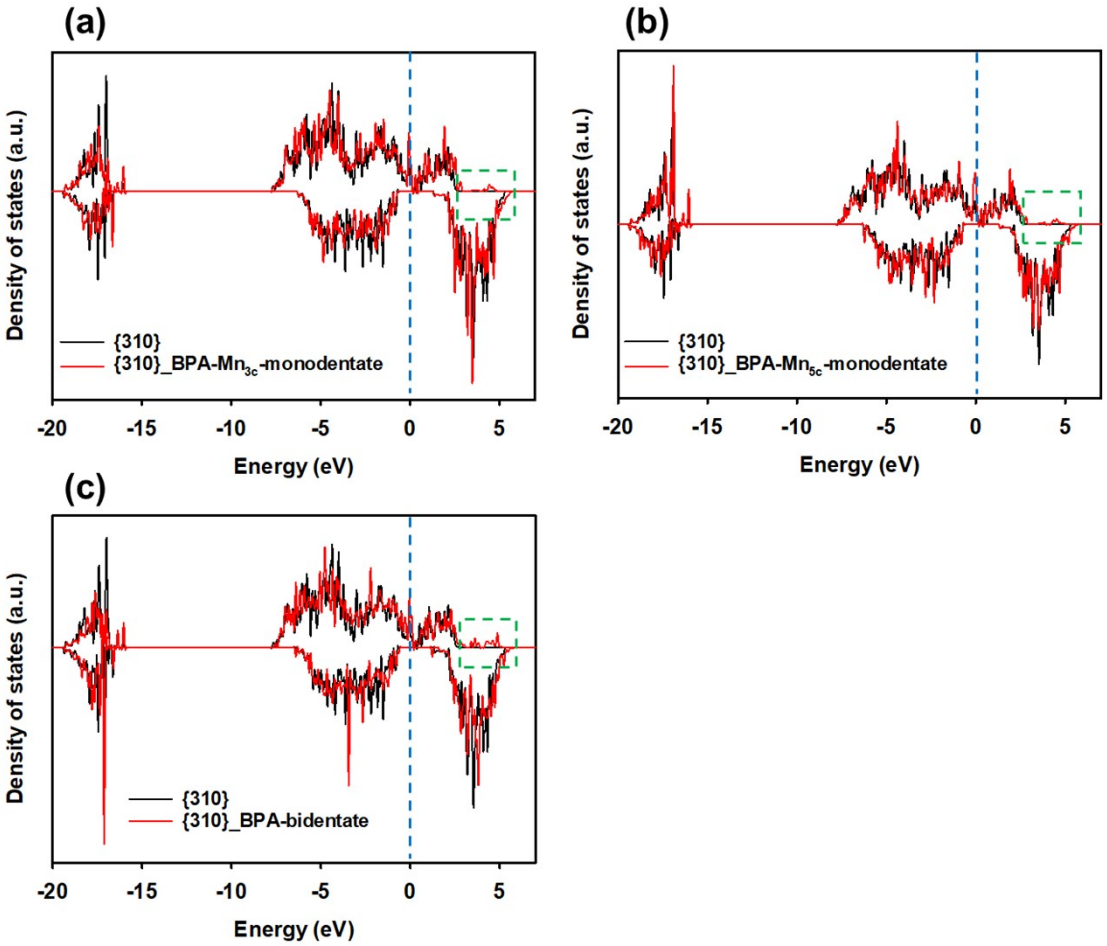

Fig. S6 Total density of states (TDOS) of α-MnO_2 surfaces exposed with the {310} facet before and after BPA adsorption in different complexation configuration: (a) monodentate coordination to Mn_{3c}, (b) monodentate coordination to Mn_{5c}, (c) bidentate coordination. The vertical blue dashed lines represent the Fermi level. New peaks (in green dashed frame) were observed at 2.5-5.0 eV in the valence band (VB) after BPA adsorption, indicating the formation of stable adsorption complexes.

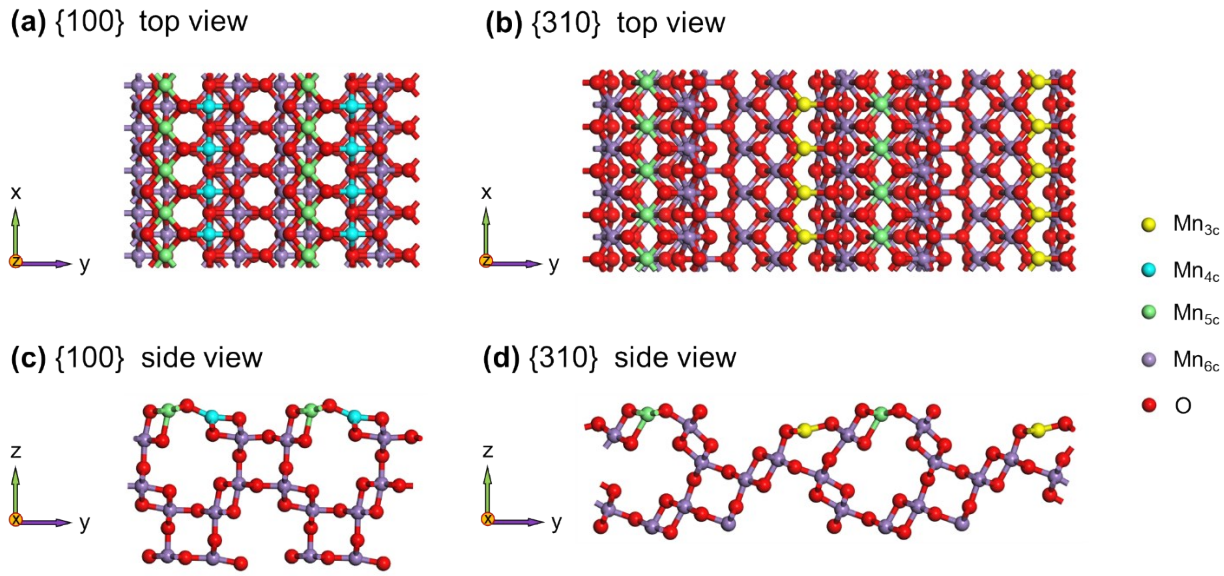

Fig. S7 (a, b) The top views and (c, d) side views of the atomic arrangement of the {100} and {310} facets of α-MnO_2, respectively. Yellow spheres are three-coordinated Mn (Mn_{3c}) atoms, blue spheres are four-coordinated Mn (Mn_{4c}) atoms, green spheres are five-coordinated Mn (Mn_{5c}) atoms, purple spheres are six-coordinated Mn (Mn_{6c}) atoms and red spheres are O atoms.

References

1 S. Rong, P. Zhang, F. Liu and Y. Yang, Engineering crystal facet of α-MnO_2 nanowire for highly efficient catalytic oxidation of carcinogenic airborne formaldehyde, *ACS Catal.*, 2018, **8**, 3435–3446.

2 P. E. Blochl, Projector augmented-wave method, *Phys. Rev. B*, 1994, **50**, 17953–17979.

3 G. Kresse and D. Joubert, From ultrasoft pseudopotentials to the projector augmented-wave method, *Phys. Rev. B*, 1999, **59**, 1758–1775.

4 A. T. Stone, Reductive dissolution of manganese(III/IV) oxides by substituted phenols, *Environ. Sci. Technol.*, 1987, **21**, 979–988.